

Secondary Geomorphic Processes and their Influence on Alluvial Fan Morphology, Channel Behaviour and Flood Hazards

Lauren Vincent¹, Brett C Eaton², Anya S Leenman², and Matthias Jakob³

¹The University of British Columbia

²University of British Columbia

³BGC Engineering Inc.

November 23, 2022

Abstract

Alluvial fans form through primary and secondary geomorphic processes. Primary processes act to transport sediment from the watershed to the fan while secondary processes re-mobilize and rework the fan surface. While primary processes on alluvial fans are well studied, secondary processes and their relationship to fan flood hazards have received little attention. The experiments described herein isolate the role of secondary processes in determining alluvial fan behaviour and morphology. We conducted four experiments, in which alluvial fans were allowed to evolve under alternating primary and secondary process periods, with different durations of secondary processes. While the secondary process duration changed, the total primary process duration remained constant keeping the total volume of sediment constant for each experimental fan. Experiments with longer durations of secondary processes generated fans with larger areas and gentler gradients. In addition, longer secondary process durations led to increased flow channelization and centralization between flood periods. These morphologic changes resulted in fewer avulsions, that occurred later during primary process periods. These results indicate that changes to the relative duration of primary and secondary process periods caused by climate change can affect fan morphology and flow behaviour.

Hosted file

agu_jgr_supporting-information_2021-07-23.docx available at <https://authorea.com/users/546570/articles/602459-secondary-geomorphic-processes-and-their-influence-on-alluvial-fan-morphology-channel-behaviour-and-flood-hazards>

Hosted file

essoar.10507644.1.docx available at <https://authorea.com/users/546570/articles/602459-secondary-geomorphic-processes-and-their-influence-on-alluvial-fan-morphology-channel-behaviour-and-flood-hazards>

Secondary Geomorphic Processes and their Influence on Alluvial Fan Morphology, Channel Behaviour and Flood Hazards

L. T. Vincent¹, B. C. Eaton¹, A. S. Leenman¹ and M. Jakob²

¹Department of Geography, University of British Columbia, 1984 West Mall, Vancouver, BC, Canada, V6T 1Z2.

²BGC Engineering Inc., 500-980 Howe Street, Vancouver, BC, Canada VCZ 0C8.

Corresponding author: Lauren T. Vincent (lauren.vincent@alumni.ubc.ca)

Key Points:

- Primary and secondary geomorphic processes respectively act to deposit and re-work material on steep alluvial fans. Primary processes have been the focus of much alluvial fan research. Our research uses physical modelling to examine the role secondary processes play in both shaping alluvial fans and determining the extent to which flood hazards may impact the fan surface.
- Changing the duration of secondary process periods on steep alluvial fans fundamentally alters fan morphology, with longer durations of secondary processes resulting in larger fans with gentler gradients. In addition, longer-lasting secondary processes generate more incised and centralized fan channels.
- The types of fan channels generated under longer secondary process periods are better able to contain and manage the hazards inherent in primary process events. Experiments with longer secondary process durations experienced fewer avulsions and a delay in the onset of avulsion during primary process periods.

Abstract

Alluvial fans form through primary and secondary geomorphic processes. Primary processes act to transport sediment from the watershed to the fan while secondary processes re-mobilize and rework the fan surface. While primary processes on alluvial fans are well studied, secondary processes and their relationship to fan flood hazards have received little attention. The experiments described herein isolate the role of secondary processes in determining alluvial fan behaviour and morphology. We conducted four experiments, in which alluvial fans were allowed to evolve under alternating primary and secondary process periods, with different durations of secondary processes. While the secondary process duration changed, the total primary process duration remained constant keeping the total volume of sediment constant for each experimental fan. Experiments with longer durations of secondary processes generated fans with larger areas and gentler gradients. In addition, longer secondary process durations led to increased flow channelization and centralization between flood periods. These morphologic changes resulted in fewer avulsions, that occurred

later during primary process periods. These results indicate that changes to the relative duration of primary and secondary process periods caused by climate change can affect fan morphology and flow behaviour.

Plain Language Summary

Alluvial fans are triangular shaped deposits of water-borne sediment at the mouth of steep creeks. Previous work on alluvial fans has focused on the processes which add material to the fan. We refer to these processes as “primary”. They encompass floods with unusually high amounts of sediment concentration and fluid landslides. Secondary processes are minor floods that rework deposited sediment on fans. While primary processes are important fan-forming events, they occur more rarely than secondary processes. In this paper, we examine how the duration of secondary processes changes the shape and size of the fan, the position of channels on the fan surface, and the behaviour of the fan during floods. We find that fans with longer durations of secondary processes were larger and less steep than those with shorter secondary process durations. The channels formed under secondary processes also better contain flow during flood events. Our results indicate that the duration of secondary processes has important effects on both the fan dimensions and their response to flood events. Climate change will alter the distribution of primary vs. secondary processes, which could have substantial impacts on how fans evolve in the future.

1. Introduction

The very nature of steep alluvial fans render them a potentially high hazard environment. Flooding on these fans is characterized by flow path uncertainty and the abrupt deposition and redistribution of sediment (Federal Emergency Management Agency, 2000). The range of geomorphic processes occurring on fans includes events with the potential to be highly destructive (Davies et al., 2013; Jakob et al., 2017; Kellerhals & Church, 1990). Paired with this, is the presence of concentrated infrastructure on alluvial fans throughout the mountainous areas of the world (T. R. Davies & McSaveney, 2008). In many parts of the world, climate change will subject both existing infrastructure and future development on fans to more frequent and catastrophic flood events in the coming century (Jakob & Lambert, 2009; Turkington et al., 2016). These factors collude to necessitate a deep risk-motivated understanding of flood processes on fans.

Flood events on fans have been studied extensively at both field (Blair & McPherson, 1994; Bull, 1977; de Haas et al., 2018) and laboratory scales (Clarke et al., 2010; Hooke & Rohrer, 1979; Schumm et al., 1987; Zarn & Davies, 1994). The majority of previous experimentation on alluvial fans and fan-deltas was completed under constant discharge to better isolate autogenic effects including avulsion characteristics (Reitz et al., 2010), channel dynamics (Kim & Jerolmack, 2008; Parker et al., 1998; Reitz & Jerolmack, 2012; Whipple et al., 1998) or spatial flood hazard distribution (Zarn & Davies, 1994). While flood intermittency has been incorporated into a number of fan-delta experiments, these

experiments focussed on impacts to sediment stratigraphy (Esposito et al., 2018) depositional lobes (Ganti et al., 2016a) and topset formation (Miller et al., 2019; Piliouras et al., 2017) without considering impacts to delta-fan flood hazard or avulsion.

Little attention has been paid to the effects of variable discharge and inter-flood periods on alluvial fan dynamics. Blair & McPherson (1994) referred to these inter-flood periods as ‘secondary processes’, describing two broad categories of processes affecting fan morphology: those processes that act to transport sediment from the watershed to the fan were classified as ‘primary’ processes while those that re-mobilize and rework sediment previously deposited on the fan were classified as ‘secondary’ processes. By varying discharge in our experiments we were able to examine the links between secondary geomorphic processes, fan morphology and fan flood hazard.

Primary processes encompass a variety of mass and water movement types, including debris floods, debris flows, hyper-concentrated flows, and mud flows, all of which act to transport material from the watershed to the fan (Pierson, 2005). These processes may be grouped by sediment concentration, velocity, water content, and typical slope gradient and may be referred to as hydrogeomorphic events (Wilford et al., 2004). Collectively, they act to construct the fan largely through aggradation, and their recurrence interval is often strongly influenced by climate, sediment availability, vegetation type and density, and weathering rates (Jakob, 1996; Webb et al., 2008). Each watershed and fan are subject to a unique set of primary processes of varying frequency, type, intensity, and magnitude.

The secondary processes described by Blair & McPherson (1994) encompass all activity that remobilizes or modifies sediment previously deposited by primary processes. These processes have been collectively referred to as fan degradation, but this classification is considered an over-simplification given the complex reworking that may occur under secondary processes. The dominant mechanism for secondary processes is fluvial transport with a sediment load below the channel’s transport capacity (Bowman, 2019).

On alluvial fans, primary and secondary processes occur on vastly different temporal scales. For example, in some arid regions fan forming processes may occur at decadal to century time scales with little secondary processes occurring in between (de Haas et al., 2014). Alternatively in humid areas primary process may occur at a frequency of 0.1 with numerous events per year classifying as secondary. Secondary processes can dominate the meso and micro scale morphology of alluvial fans because of the higher cumulative geomorphic work accomplished by high frequency secondary processes (de Haas et al., 2014). Among the surface morphology features indicating the dominance of secondary processes are channel entrenchment and up-fan migration of the incision point (Bowman, 2019).

Secondary processes have a profound impact on fan morphology but remain

under-represented in alluvial fan experiments. Much of the laboratory experimental work on steep alluvial fans has used primary processes only, often at constant discharge and sediment feed. The increased channelization and entrenchment of flow on fans during secondary processes can contain consequent aggradational events and shift flood hazards down-fan (Wasklewicz & Scheinert, 2016).

We hypothesize that prevailing secondary processes contain and reduce debris-flood hazards on alluvial fans. We test this hypothesis using physical laboratory-scale modelling.

1. Experimental Design

Physical models have long been used in alluvial fan research, with experimental studies beginning in the 1960s (Hooke, 1967, 1968). Physical models are important tools in the observation of natural processes because they allow for isolation and examination of the effects of single factor changes, allowing for predictive insight through analysis (Paola et al., 2009). Experimentation using physical models is useful for alluvial fan systems, as it allows for observations on temporal scales consistent with fan evolution (Clarke et al., 2010; Harvey, 2010).

1. Model Setup

We conducted our experiments using the physical model of a generic gravel-cobble fan described by Leenman & Eaton (2021). The experimental setup consisted of a 2.44 x 2.44 m stream table with 0.3 m high walls, with a 0.2 m wide, 0.5 m long inlet channel at one corner (Figure 1). The inlet channel represented a short section of a confined stream channel upstream of the fan apex which was narrowed to 0.071 m at the fan apex. The table was set to an angle of 0.0002 m m^{-1} (0.02%) with the inlet at the highest corner, and a vertical drain at the lowest corner. A sediment feeder was mounted above the upstream end of the inlet channel. Water was input from a constant head tank with an adjustable outflow. Sediment was allowed to aggrade and degrade freely in the inlet channel, as in a natural system. The water used in the experiments was dyed blue to allow photos to be used for automated channel mapping.

We used a sediment mixture ranging between 0.25 and 2.8 mm to create more visually realistic channels (Hamilton et al., 2013). The mixture was truncated at 0.25 mm to maintain a hydraulically rough boundary, but otherwise reflects a scaled distribution of sediment sampled from the surface of Three Sisters Creek fan in Canmore, Alberta, Canada in July, 2018 (Figure 2). This grain size distribution is characteristic of numerous fans in the Canmore area (BGC Engineering Inc., 2014, 2016). The cut-off sediment size corresponds to a prototype value of about 32 mm, which represents a significant proportion of the field GSD (approx. 42%). The truncation results in the deviation between experimental and prototype GSD for smaller grain sizes. From the GSD scaling, the length scale for this generic model is 1:128. The median size of the model bed material

of 0.6 mm corresponds to a prototype value of 77 mm, and the model D_{84} of 1.3 mm corresponds to a prototype value of 166 mm.

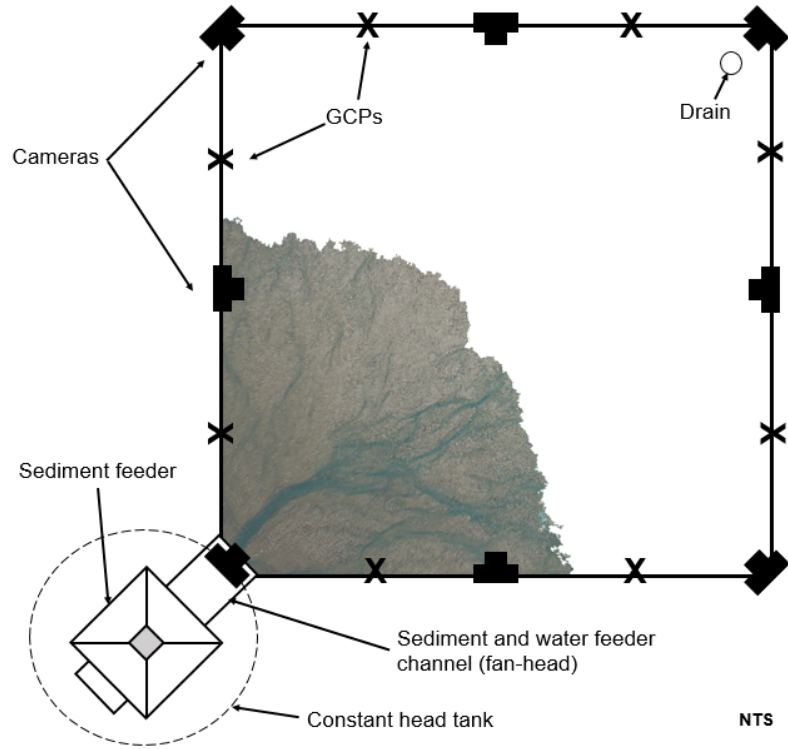


Figure 1. The idealized experimental setup. GCP = ground control point (used to georeference photographs). An orthorectified image of a typical fan is shown in the background.

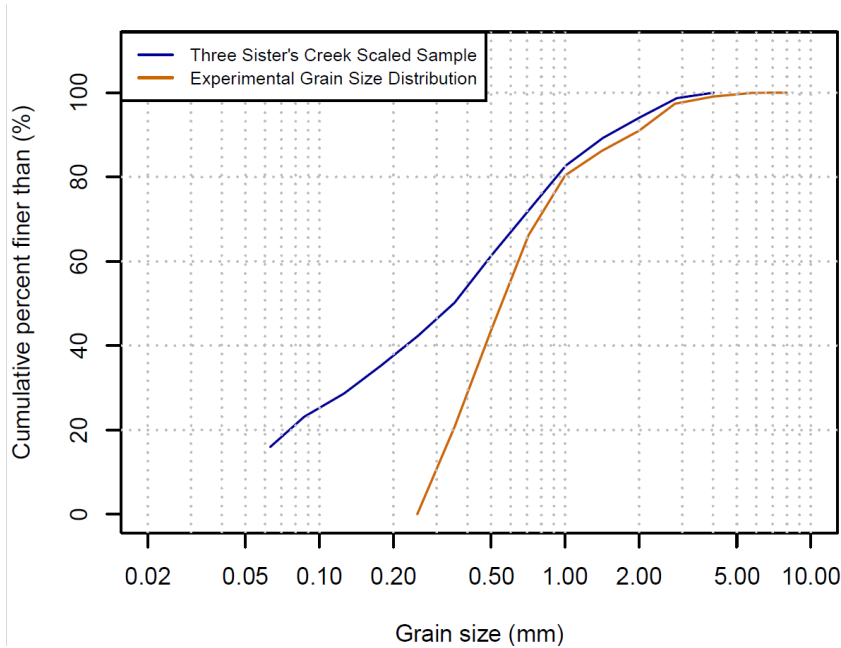


Figure 2. Comparison of scaled field and experimental grain size distributions.

In part due to the imperfect representation of the prototype grain size distribution, our experiments are best described as mobile-bed “similarity of process” models (Hooke, 1968). While the model is geometrically scaled, it does not abide by strict Froude-scaling rules due to the presence of transitional and laminar flow. The width of the channels and the gradient of the fan were self-formed, with gradients between 0.06 and 0.12 m m⁻¹. As such, it was impossible to experimentally control the Froude number, mean channel width, or mean hydraulic depth for the experiments; they were considered emergent properties of the experiments.

The process-similar approach used to generate alluvial fan morphology in our experiments was first developed by Hooke (1968) and has a basis in micro-scale modelling (Davies et al., 2003; Malverti et al., 2008). The broad morphologic processes present on natural fans are represented in our experiments. However, the length ratio of 1:128 – while enabling experiments on fan evolution – makes it difficult to establish dynamic similarity, meaning the ratios of masses and ratios of forces between the natural fan and the experiment may not be preserved.

1. Experiments

Our experiments are divided into two distinct phases: fan formation (Phase 1) and flooding (Phase 2). In Phase 1, we generated alluvial fans with alternating primary and secondary process inputs. In the second phase, the fans were then subjected to a sequence of flood events of varying magnitudes (i.e. primary process events) to study how the fan morphology affected flood hazards, in detail.

A summary of the complete sequence of floods run for two of the experiments is shown in Figure 3. Primary processes in Phase 1 used a discharge of 100 ml/s and a sediment feed of 10 g/s (Table 1). This reflects a sediment concentration of 10% which is typical of what might be expected during a debris flood (Church & Jakob, 2020; Pierson, 2005). Throughout our experiments, primary processes – also referred to as flood periods – are debris floods as per Church and Jakob’s (2020) definition. Secondary processes used a discharge of 50 ml/s and no sediment feed. This reflects a discharge at which low rates of sediment transport were observed on the fan surface, and follows discharge ratios similar to those seen in other fan-delta and river plume experiments (Chatanantavet & Lamb, 2014; Miller et al., 2019; Piliouras et al., 2017).

For each experiment, primary processes were run for a total of 120 minutes, resulting in 72 kg of sediment being discharged onto each experimental fan. This allowed for multiple cycles of channel avulsion and surface reworking, and permitted observations of fan evolution processes. We ran four experiments with the same duration of primary process inputs, or flood periods, and increasing durations of secondary processes, or inter-flood periods. This resulted in experiments with longer durations of secondary processes having a longer total experiment duration (see ‘Total duration’ in Table 1). In the second phase, the fans generated during fan formation were subjected to the flood sequence summarized in Table 2.

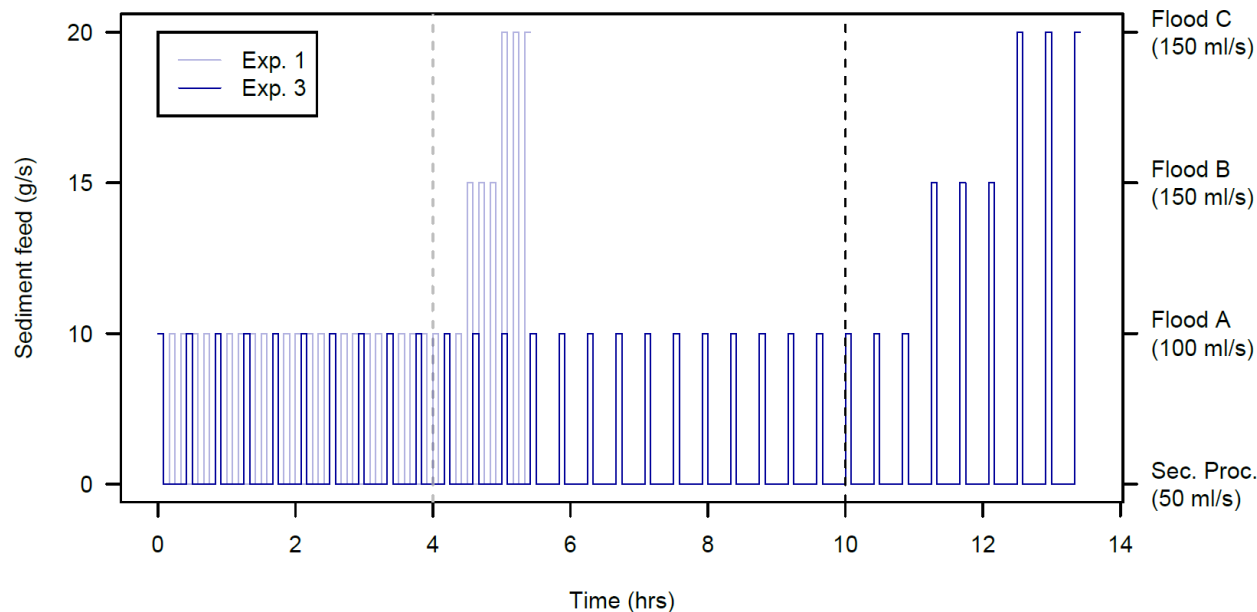


Figure 3. An example of the flood sequence for two complete experiments, including Phase 1: fan formation and Phase 2: fan flooding. As per Table 1, Experiment 1 has 5 minute periods of secondary processes while Experiment

3 has 20 minute periods of secondary processes. The dashed grey and black lines show the transition from Phase 1 to Phase 2 for Experiments 1 and 3, respectively.

Table 1. Summary of Experimental Inputs for Fan Formation (Phase 1).

Experiment number	Primary processes		Secondary processes		
	Discharge (ml/s)	Sediment feed (g/s)	Duration (mins)	Discharge (ml/s)	Sediment feed (g/s)
1	100	10	5	50	0
2	100	10	5	50	0
3	100	10	5	50	0
4	100	10	5	50	0

Table 2. Summary of Experimental Inputs for Fan Flooding (Phase 2).

Flood name	Discharge (ml/s)	Sediment feed (g/s)	Duration (mins)	Number of repeats
A	100	10	5	3
B	150	15	5	3
C	150	20	5	3

1. Data Collection and Analysis

Fan topography and flow patterns were monitored using Structure from Motion (SfM) photogrammetry. SfM has been used for various geoscientific approaches, and has recently been used in physical models (Leduc et al., 2019; Morgan et al., 2017). Photographic data were collected using nine Canon EOS Rebel T6 digital single-lens reflex cameras positioned over the experimental setup (Figure 1). Eight of the cameras were positioned at equally spaced intervals around the perimeter of the stream table, and the ninth camera was mounted perpendicular, face down above the experiment at a height of 1.8 m. The cameras collected synchronous images of the experimental fans at one minute intervals.

The resulting images were georeferenced to a local coordinate system at each time step using eight ground control points (GCPs) on the stream table walls. The images were then processed in AgiSoft Photoscan (AgiSoft, 2018) to produce point clouds ($\sim 280,000$ points per m^2) and orthomosaics (1 mm resolution). The topographic point clouds were used to generate digital elevation models (DEMs). In order to generate DEMs with 1 mm resolution, topographic point clouds were interpolated using a k-nearest neighbours approach (number of neighbours = 2), combined with inverse distance weighting (power = 2). DEMs were cropped to 1 cm from the edges of the table to remove any edge effects. The DEM processing and analysis were completed in R (R Core Team, 2019) using functions from the lidR package (Roussel & Auty, 2020).

Using functions from the raster package (Hijmans et al., 2020), the initial ($t =$

0) DEM was subtracted from each subsequent DEM. This produced a surface of elevation change relative to the initial, empty table. To determine the extent of the fan at each time step, the output was thresholded at 6 mm. With the largest grains in the experiment ranging between 5.8 and 8 mm, this threshold was used to differentiate between portions of the fan table with, and without, sediment buildup between the timestep of interest and $t = 0$. Cells with > 6 mm of elevation increase were assigned a value of 1, while those with < 6 mm of increase were assigned a value of 0, to produce a map of the fan area.

We used topographic change detection to generate DEMs of Difference (DoDs) using an error threshold of 2 mm. Previous work by Leenman (2021) found that within the flow map area, the mean elevation difference (wet - dry) was 1.6 mm (standard deviation of 1.2 mm), while outside the flow map area, the mean elevation difference (wet - dry) was 1.1 mm (standard deviation of 0.9 mm). Together, the DoDs, orthomosaics, and DEMs formed the primary data from which all further analysis described herein was conducted. Additional details on the experimental apparatus and data collection methods are included in Leenman & Eaton (2021).

1. Results

(a) Fan Morphology

The DEMs described in Section 3 were used to characterize fan gradient from fan apex to fan toe along a series of 88 profiles at intervals of 1 degree; profiles along the table walls were excluded. Fan elevation was extracted at 1 mm intervals along each profile and a linear regression of elevation and distance values along each profile was conducted to calculate fan gradient. Figure 4 shows the mean fan gradient, averaged over each of the 88 profiles, at each time step of the experiments. The results are plotted over normalized time, t^* , to account for the different experimental durations.

Fan gradient achieved a lower equilibrium value with longer durations of secondary process action; on average approximately 0.1 m m^{-1} for Experiment 1 and 0.06 m m^{-1} for Experiment 4. Since the same quantity of sediment was discharged onto each fan, fans with shallower gradients had correspondingly larger areas. In other words, longer durations of secondary processes generated larger, gentler fans. The abrupt decrease in fan gradient at $t^* = 0.58$ seen in Experiment 1 was related to a temporary sediment blockage. Results for a repeat of Experiment 1, Experiment 1B, are included in the supporting information (Figure S1).

Throughout our experiments, fan gradient decreased over time before asymptotically approaching a dynamic equilibrium. This dynamic equilibrium was characterized by fan gradient oscillating around a relatively constant value, where the oscillations were a result of alternating primary and secondary processes. These oscillations, or sawtooth patterns, in mean fan gradient were closely tied to primary and secondary process periods for all experiments. The peaks (i.e. higher gradients) in this pattern corresponded approximately to primary process

periods when sediment was being added to the fan, while the lower gradients corresponded to secondary process periods. Although the sawtooth pattern was visible in all experiments, the pattern was most regular and most consistently linked with primary process periods in Experiment 4.

Mean fan gradient was also plotted by fan azimuth to assess differences in gradient across the fan surface. In Figure 5 the gradient along a given fan axis-to-toe profile was averaged over the complete duration of the experiment. In our experiments, alluvial fan gradient varied by azimuth; fan gradient was highest near the flanks of the fan and gentlest along the fan axis. Similar results were found by Hooke & Rohrer (1979) and Zarn & Davies (1994). This pattern was particularly pronounced for Experiments 3 and 4, with the highest durations of secondary processes. That changes in mean fan gradient were observed over time periods as short as 5 minutes indicates the profound topographic effects of secondary processes. In short, the spatial and temporal variations in fan gradient point to the importance of secondary process duration as an allogenic forcing on fan morphology.

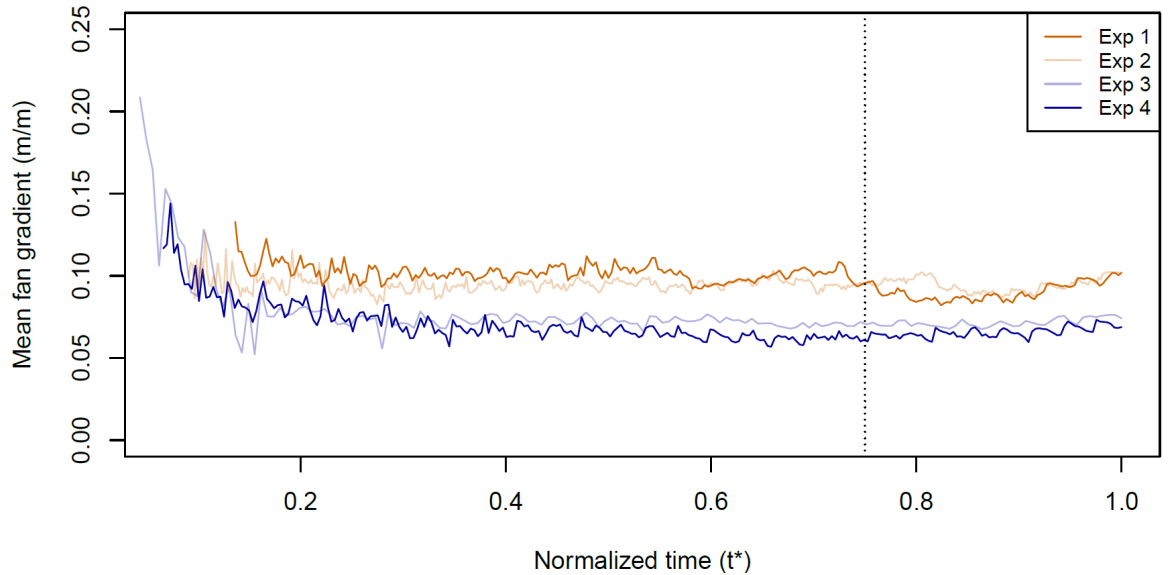


Figure 4. Mean fan gradient over normalized time for each of the four experiments. The dashed black line shows the approximate point of transition from Phase 1, fan formation, to Phase 2, fan flooding. The higher variability in gradients for $t^* < 0.2$ likely stems from measurement error when the fan was very small.

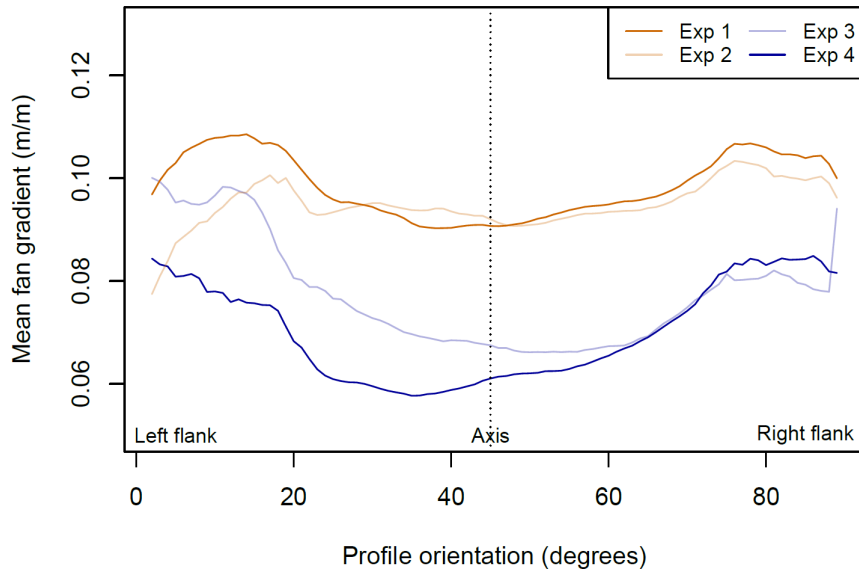


Figure 5. Mean fan gradient along each of the fan profiles. Profile orientation in degrees is measured from the left flank of the fan. Note that some spurious gradient measurements (e.g. abrupt changes in gradient) may exist near the walls of the experiment.

1. Channel Pattern and Incision

The images taken throughout our experiments were used to generate orthomosaics (Section 3) from which we created maps showing the location of flow/channels on the fan surface. This was done to study channel pattern and incision for the different experiments. Because the water used had been dyed blue to differentiate it from the fan sediment, a colour threshold was used to delineate channels on the fan surface. Values greater than the colour threshold were assigned a value of 1, and those less than or equal to the threshold were assigned a value of 0, resulting in a binary map of channel vs non-channel locations (examples shown in Figure 6). These maps were smoothed with a 7x7 cell majority filter and wet patches smaller than 10 cm^2 were removed.

Using the binary channel maps, the wet area data were normalized by total fan area to give the fan wet fraction, thereby accounting for different fan dimensions across experiments. The wet fraction of the fan, or the proportion of the fan inundated by flow, was calculated at each time step of the experiments. The wet fraction generally ranged from 14% and 32% throughout our experiments, and abrupt changes to fan wet fraction within this range could be used as a proxy for changes in channel pattern. For example, the images shown in Figure 6, taken ten minutes apart, reflect wet fractions of 15% and 22%, for a and b respectively. In general, more channelized flow resulted in lower fan wet fractions (6a) while more dispersed channels resulted in higher fan wet fractions (6b).

This relationship between wet fraction and characteristic fan channel patterns allowed for rapid characterisation of flow patterns across flood and inter-flood periods in our experiments.

To visualize the differences between Phase 2 wet fractions for the four experiments, the data were grouped by experiment and separated into flood and pre-flood values. A box plot showing fan wet fraction prior to flooding and during flooding is shown for each experiment in Figure 7. Although the flood wet fractions did not differ significantly across the four experiments, there was a visible difference between the pre-flood wet fractions for the four experiments. Experiments 1 and 2 had similar pre-flood wet fractions, while Experiment 3 and Experiment 4 had progressively lower pre-flood wet fractions.

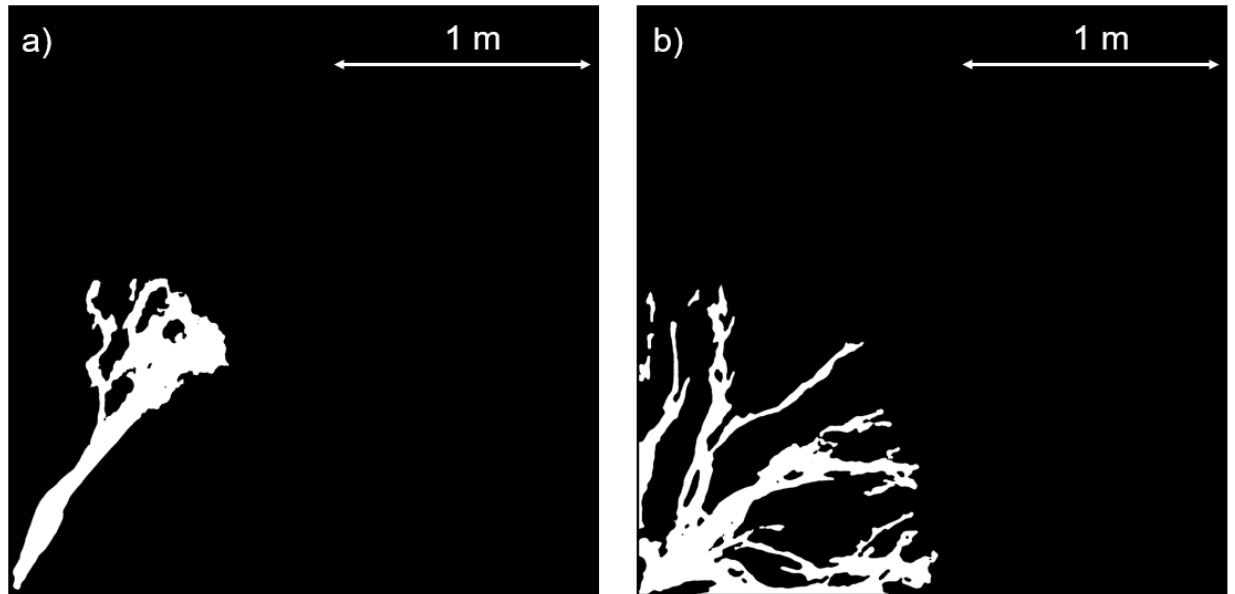


Figure 6. Example of binary channel maps taken from Experiment 4 at (a) $t = 20$ h 55 min during a secondary process period demonstrating channelized flow and (b) $t = 21$ h 05 min during flooding (primary processes) demonstrating dispersed flow. White pixels indicate fan channels, or wet areas, while black pixels reflect dry areas.

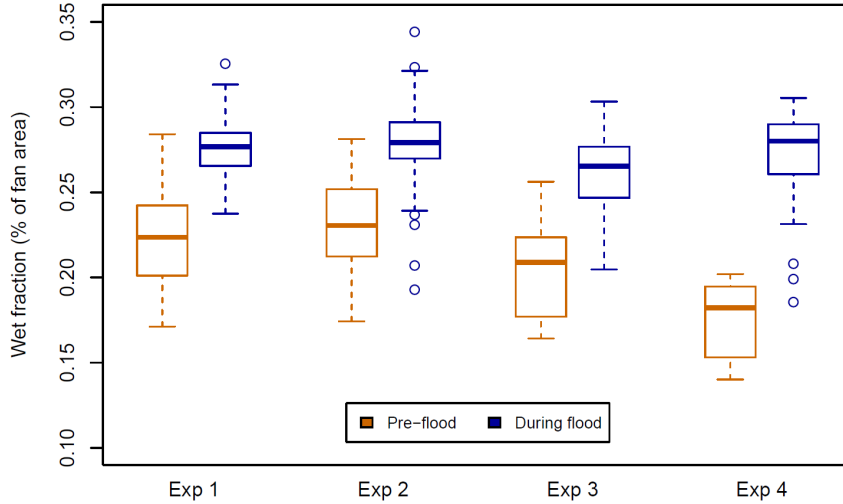


Figure 7. Box plot showing the differences in wet fraction for the pre-flood and flood time-steps for the four experiments. The boxes delineate the inter-quartile range, while the whiskers reflect the minimum and maximum values excluding outliers which are represented as open circles. The data shown here are from Phase 2. ‘During flood’ values were averaged over the five minute flood duration for each of the nine flood events in Phase 2. ‘Pre-flood’ values were taken from the minute prior to the onset of flooding.

Prior to the onset of flooding, the number of channels decreased with increasing secondary process duration, with Experiment 4 only having one channel on average (Table 3). This explains the notable decrease in pre-flood wet fraction in Figure 7. That flow in Experiment 4 was confined to a single channel prior to flooding indicates the power of secondary processes in governing pre-flood conditions. All our experiments averaged approximately two channels during flooding. The number of fan channels increased as flooding progressed with a maximum of four and three distinct channels during and prior to flooding, respectively.

Throughout our experiments, fan channels diverted toward the fan edges at the onset of flooding, and gradually re-centralized during secondary process action, leading to the characteristic channel patterns exemplified in Figure 6. The fan wet fraction allowed for rapid characterization of fan channel patterns throughout the experiments. Figures 6a and 6b show typical fan channel patterns under secondary and primary processes, respectively.

1. Avulsion

Following the definitions of Allen (1965) and Ganti et al. (2016b), we characterized avulsions as sudden changes in channel position, as it is these kinds of abrupt channel changes that may increase the potential for flood damage and

building impact (Federal Emergency Management Agency, 2000; French, 1987). For our experiments, a channel was defined as any continuous wet portion of the fan surface whose source was traceable to the fan apex.

We conducted a manual analysis of avulsion frequency over Phase 2 of the experiments wherein avulsions were characterized visually at one-minute intervals using the orthomosaics. The characterization of avulsion frequency was limited to Phase 2 in part to limit the scope of the analysis and in part to compare avulsion characteristics across the different Phase 2 flood events. Avulsions occurring within 0.25 m of the fan apex, i.e. the top 35 - 50% of the fan by radius, were included. Avulsions occurring on more distal, minor fan channels were not included in this analysis. To eliminate bias, the results of the manual avulsion assessment were validated with an automated analysis which used the binary channel maps to chart abrupt changes in channel patterns. Although the automated method was more sensitive to channel shifting than the manual method, both methods identified many of the same avulsion events (+/- 5 minutes).

Avulsion became less frequent with increasing duration of secondary processes (Table 3). Our manual avulsion count indicated that in Phase 2, 20 avulsions occurred in Experiment 1, while only 12 avulsions occurred during Experiment 4. In addition, the time at which the avulsions first occurred was earliest for Experiment 1 and latest for Experiment 4. That is, avulsion occurred both sooner after the onset of flooding and more frequently in experiments with shorter secondary process duration. In a non-laboratory setting this implies that high frequency debris-flow or debris-flood creeks are more likely to avulse than in low frequency systems. In Table 3, avulsion timing refers to the minute of flooding in which avulsion first occurred, with $t = 0$ indicating the onset of flooding or primary processes. Percent change reflects the percentage of observed avulsions in excess of or fewer than predicted avulsions (Reitz et al., 2010).

While avulsions occurred during each of the three flood sequences, the avulsion count was highest for Flood C (Table 3) which had the greatest input sediment concentration (~ 13%). This aligns with previous work suggesting that avulsion frequency is proportional to sediment concentration (Ashworth et al., 2004; Bryant et al., 1995; De Haas et al., 2016; Reitz et al., 2010). It is also intuitive as higher sediment concentrations both increase flood stage because of the flow bulking but also encourage differential channel bed aggradation which further jeopardizes freeboard (Church & Jakob, 2020; Jakob & Church, 2020).

While Experiments 1 and 2 had the greatest number of avulsions during Flood C, Experiment 3 had the greatest avulsion count during Flood B and Experiment 4's avulsions were equally distributed across all three flood types. Although it is difficult to extract definite conclusions from these limited data, it is plausible that longer durations of secondary processes in Experiments 3 and 4 countered avulsion tendency under increased sediment concentration. This may be attributed to the reworking of erodible sediments in floods towards the distal portions of the fan which is accompanied by fan incision. This phenomenon has

- 7%

4 & 1.0 & 1.9 & 3.4 & 4 & 4 & 4 & 12 & 16 &

- 33%

1. Discussion

In our experiments, the duration of secondary processes had a profound impact on both fan morphology and behaviour during floods. Each of the four fans was created with the same volume of sediment; the only difference was the duration of secondary processes between each flood. Secondary processes were run for periods of 5, 10, 20, and 40 minutes for Experiments 1, 2, 3, and 4, respectively.

Longer durations of secondary processes generated larger, less steep fans. They also concentrated flow along the fan axis, where a single channel often formed during secondary processes. These channels tended to be more incised and centralized under longer secondary process durations.

The channels formed under secondary processes were further incised into the fan surface. Terraced banks formed along these channels; visual observations revealed increased incision depths under longer durations of secondary processes. DEMs indicated that channels were most incised in Experiment 4 (40 min duration), up to depths of 1 cm. This measurement was likely an underestimate of true channel incision as refraction at the water surface tended to reduce channel depth estimates.

Re-centralization and straightening of fan channels increase channel efficiency (Graf & Blanckaert, 2002; Pacheco-Ceballos, 1984), in turn, the efficiencies of these centralized channels allowed for the transport of additional sediment, thereby reducing fan gradient along the axis and leaving gradients along the fan flanks unaltered. Primary processes dominantly acted along the fan flanks, depositing sediment, while secondary processes dominantly acted along the fan axis, eroding sediment (see Figure S2, supporting information).

Centralization of flow through secondary processes is thought to be the driver of increased cross-fan gradient differences in the Experiment 3 and 4 profiles (Figure 5) and the decreased pre-flood wet fraction for Experiments 3 and 4 (Figure 7). In addition, channel incision and the restriction of flow on the fan surface were the likely causes of decreased avulsion frequency, and delayed avulsion timing in experiments with longer secondary processes.

Figure 8 summarizes the differences in fan and channel morphology under differing durations of secondary processes. Fan A was formed under shorter secondary processes durations (Experiment 1) while Fan B was formed under longer secondary process durations (Experiment 4). Fan A is smaller and steeper. Numerous braided channels are present on the surface of Fan A and there is negligible

channel incision. The intersection point (where an incised channel reaches the fan surface) is located approximately half way down-fan from the apex. Conversely, Fan B is larger and has a shallower gradient. It has a single channel which is entrenched, and the intersection point is located further from the fan apex, in the bottom third of the fan.

The larger area and lower gradient give Fan B a greater potential for energy dissipation during flood events. In addition, the single-thread channel allows for greater containment of flood events and may serve to delay avulsion onset and decrease avulsion frequency. The results of this research indicate that Fan B is more resilient to floods and does not experience significant changes to overall gradient and area when subjected to flooding. Nevertheless, despite these differences in flood response, our data suggest that a similar fraction of Fan A and Fan B may become inundated during a flood event.

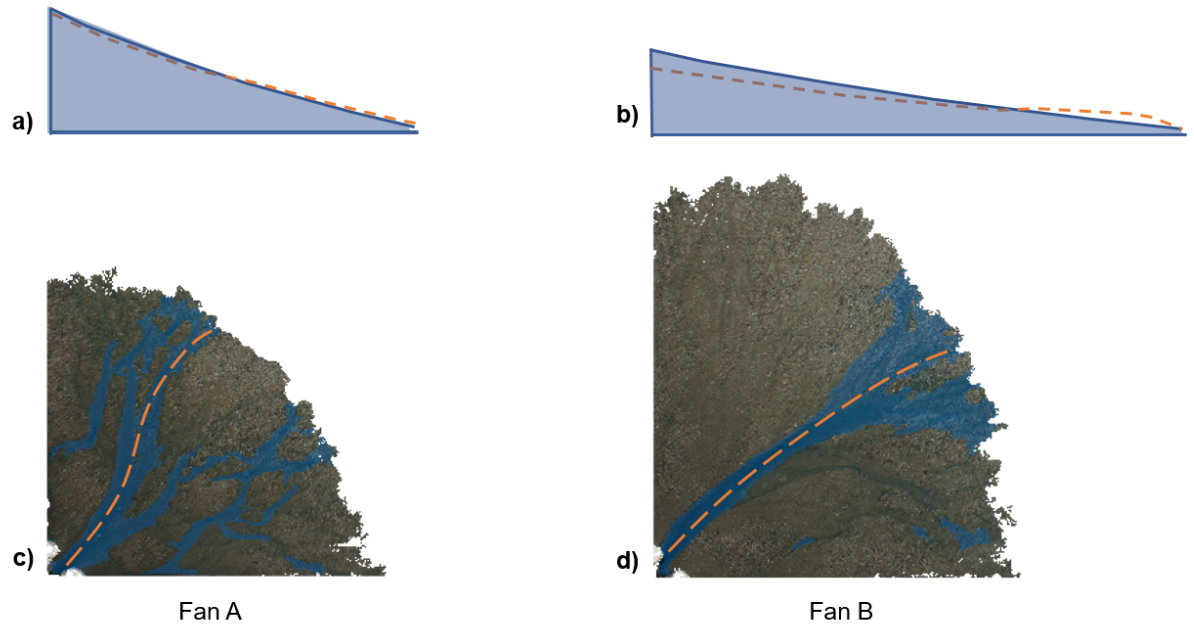


Figure 8. Summary of secondary process effects on fan morphology with two fans formed under (c) shorter and (d) longer durations of secondary processes. The primary fan channel on each of the fans is indicated by a dashed orange line and a hypothetical cross-section for each of these channels (a, b) is shown above the fans. The image of Fan A was taken at $t = 3$ h 30 min during Experiment 1, while the image for Fan B was taken at $t = 16$ h 25 min during Experiment 4.

Climate and sediment availability exert a strong influence over the recurrence interval of primary processes (Bovis & Jakob, 1999; Jakob, 1996; Webb et al.,

2008). In many places, changes in precipitation are predicted to increase the frequency and magnitude of extreme geomorphic events in the coming century (Jakob & Lambert, 2009; Jakob & Owen, 2021; Turkington et al., 2016). The increased recurrence interval of these events may decrease the time over which secondary processes are able to act on alluvial fans, potentially shifting the balance of aggradation and entrenchment on fan surfaces in the future.

For fans with supply unlimited (Jakob, 1996, 2021) source basins, climate change will likely result in a greater frequency of primary processes arriving at the fan apex. Such an increase in primary process events would be expected to shift the fan morphology and behaviour towards that of Fan A. For sediment supply-limited fans, the frequency of debris flows (primary process) will likely increase but with decreasing sediment volumes attributable to the lesser time available for channel sediment recharge. In addition to climate change, other variables such as land use change, forest fires, or increased landslide activity in the watershed may alter the balance of primary and secondary processes acting on the fan. The impacts of these changes on fan morphology will need to be investigated through further experimentation and field studies.

While the boundaries between primary and secondary processes were clear in the controlled environment of our experiments, differentiation between these geomorphic processes is more complex on natural fans. In the case of debris flows, entrenchment may be initiated by the less viscous tail, or afterflow, typically following the surge front (Iverson, 1997; Jakob et al., 2013; Takahashi, 2014). This was the case at Neff Creek, where channel erosion was thought to have begun during the debris flow itself. Ultimately, the afterflows of the primary process event resulted in vertical erosion of the channel to depths of 14 m (Lau, 2017) indicating that channel incision is not the domain of secondary processes alone. The complete separation of primary and secondary geomorphic processes on natural fans is not possible. While our results provide general conclusions on the impacts of these processes, this complexity should be considered when interpreting results at the event scale.

1. Conclusion

Despite several decades of alluvial fan experimentation and research, the focus has remained on primary fan-forming processes. The role of inter-event, or secondary, processes on fan evolution and behaviour has largely been neglected. The objective of this study was to advance our understanding of secondary processes on steep alluvial fans. This was achieved through four experiments designed to isolate the impacts of secondary process duration. The results presented herein yield insight into the emergent properties of the fan system under different secondary process conditions.

This study suggests that:

1. Fan morphology may be strongly influenced by secondary process duration. In our experiments, fans formed under longer durations of secondary processes were larger and had gentler gradients.

2. Pre-flood conditions including channel incision and centralization of flow paths act to contain primary process events by channelizing floods and decreasing the overall fan wet fraction. Pre-flood conditions are therefore important determinants of fan flood hazards associated with primary processes.
3. A shift towards decreased secondary process durations results in increased avulsion frequency and earlier avulsions during flood events. Conversely, increasing length of secondary processes delays avulsions and reduces their frequency.

The results highlight the importance of understanding antecedent morphologic fan conditions in estimating the overall flood impact. While our results hold true in an experimental setting, much work remains to support these data with detailed long-term observations on fan adjustments during and after primary and secondary fan processes. Scaling limitations must be considered when interpreting our results; in particular, extrapolations of rates and volumes of sediment transport measured in our model should be validated against field data from the fan of interest.

Acknowledgments, Samples, and Data

Purchase of equipment and construction of the experiment were funded by an NSERC Discovery Grant to B. Eaton. The authors have no conflicts of interest to declare. The source data used to generate DEMs and binary channel maps for this study are stored on the Federated Research Data Repository (FRDR) via the identifier 10.20383/102.0480 and are associated with ORCID iD <https://orcid.org/0000-0002-5118-9849>*

**Please note that at the time of submission the data are in the process of being uploaded.*

References

- AgiSoft. (2018). *AgiSoft PhotoScan Professional*. Retrieved from <http://www.agisoft.com/downloads/installer/>
- Allen, J. R. L. (1965). A Review of the Origin and Characteristics of Recent Alluvial Sediments. *Sedimentology*, 5(2), 89–191. <https://doi.org/10.1111/j.1365-3091.1965.tb01561.x>
- Ashworth, P. J., Best, J. L., & Jones, M. (2004). Relationship between sediment supply and avulsion frequency in braided rivers. *Geology*, 32(1), 21–24. <https://doi.org/10.1130/G19919.1>
- BGC Engineering Inc. (2014). *Three Sisters Creek Debris-Flood Hazard Assessment*. Prepared for the Town of Canmore.
- BGC Engineering Inc. (2016). *Three Sisters Creek Debris Flood Mitigation Modelling*. Prepared for the Town of Canmore.
- Blair, T. C., & McPherson, J. G. (1994). Alluvial fans and their natural distinction from rivers based on morphology, hydraulic processes, sedimentary processes, and facies assemblages. *Journal of Sedimentary Research A: Sedimentary Petrology & Processes*, A64(3), 450–489.
- Bovis, M. J., & Jakob, M. (1999). *THE ROLE OF DEBRIS SUPPLY CONDITIONS IN PREDICTING DEBRIS FLOW ACTIVITY*.

1054, 1039–1054. Bowman, D. (2019). Principles of Alluvial Fan Morphology. In *Principles of Alluvial Fan Morphology*. <https://doi.org/10.1007/978-94-024-1558-2> Bryant, M., Falk, P., & Paola, C. (1995). Experimental study of avulsion frequency and rate of deposition. *Geology*, *23*(4), 365–368. Bull, W. B. (1977). The alluvial-fan environment. *Progress in Physical Geography*, *1*(2), 222–270. Chatanantavet, P., & Lamb, M. P. (2014). Sediment transport and topographic evolution of a coupled river and river plume system: An experimental and numerical study. *Journal of Geophysical Research: Earth Surface*, *119*, 1263–1282. <https://doi.org/10.1002/2013JF002810> Church, M., & Jakob, M. (2020). What Is a Debris Flood? *Water Resources Research*, *56*, 1–17. <https://doi.org/10.1029/2020WR027144> Church, & Ryder, J. M. (1972). Paraglacial Sedimentation: A Consideration of Fluvial Processes Conditioned by Glaciation. *Geological Society of America Bulletin*, *83*(10), 3059–3072. Clarke, L., Quine, T. A., & Nicholas, A. (2010). An experimental investigation of autogenic behaviour during alluvial fan evolution. *Geomorphology*, *115*(3–4), 278–285. <https://doi.org/10.1016/j.geomorph.2009.06.033> Davies, McSaveney, M. J., & Clarkson, P. J. (2003). Anthropogenic aggradation of the Waiho River, Westland, New Zealand: Microscale modelling. *Earth Surface Processes and Landforms*, *28*(2), 209–218. <https://doi.org/10.1002/esp.449> Davies, Phillips, C., & Warburton, J. (2013). Processes, Transport, Deposition, and Landforms: Flow. In J. Shroder (Editor-in-chief), R. A. Marston, & M. Stoffel (Eds.), *Treatise on Geomorphology* (7th ed., Vol. 7, pp. 158–170). <https://doi.org/10.1016/B978-0-12-374739-6.00160-3> Davies, T. R., & McSaveney, M. J. (2008). Principles of sustainable development on fans. *Journal of Hydrology (NZ)*, *47*(1), 43–65. de Haas, T., Densmore, A. L., Stoffel, M., Suwa, H., Imaizumi, F., Ballesteros-Cánovas, J. A., & Wasklewicz, T. (2018). Avulsions and the spatio-temporal evolution of debris-flow fans. *Earth-Science Reviews*, *177*(November 2017), 53–75. <https://doi.org/10.1016/j.earscirev.2017.11.007> De Haas, T., Van Den Berg, W., Braat, L., & Kleinhans, M. G. (2016). Autogenic avulsion, channelization and backfilling dynamics of debris-flow fans. *Sedimentology*, *63*(6), 1596–1619. <https://doi.org/10.1111/sed.12275> de Haas, T., Ventra, D., Carbonneau, P. E., & Kleinhans, M. G. (2014). Debris-flow dominance of alluvial fans masked by runoff reworking and weathering. *Geomorphology*, *217*, 165–181. <https://doi.org/10.1016/j.geomorph.2014.04.028> Esposito, C. R., Di Leonardo, D., Harlan, M., & Straub, K. M. (2018). Sediment Storage Partitioning in Alluvial Stratigraphy: The Influence of Discharge Variability. *Journal of Sedimentary Research*, *88*(6), 717–726. <https://doi.org/10.2110/jsr.2018.36> Federal Emergency Management Agency. (2000). *Guidelines for Determining Flood Hazards on Alluvial Fans*. Washington, D.C. French, R. H. (1987). Hydraulic Processes on Alluvial Fans. In *Elsevier Science Publishing Company Inc.* (1st ed.). [https://doi.org/10.1016/S0167-5648\(08\)70007-8](https://doi.org/10.1016/S0167-5648(08)70007-8) Ganti, V., Chadwick, A. J., Hassenruck-Gudipati, H. J., Fuller, B. M., & Lamb, M. P. (2016a). Experimental river delta size set by multiple floods and backwater hydrodynamics. *Science Advances*, *2*(5), 1–11. <https://doi.org/10.1126/sciadv.1501768> Ganti, V., Chadwick, A. J., Hassenruck-Gudipati, H. J., Fuller, B. M., & Lamb, M. P. (2016b). Experimental river delta

size set by multiple floods and backwater hydrodynamics. *Science Advances*, 2(5). <https://doi.org/10.1126/sciadv.1501768>Graf, W. H., & Blanckaert, K. (2002). Flow around bends in rivers. *2nd International Conference New Trends in Water and Environmental Engineering for Safety and Life: Eco-Compatible Solutions for Aquatic Environments*, 1–9.Hamilton, P. B., Strom, K., & Hoyal, D. C. J. D. (2013). Autogenic incision-backfilling cycles and lobe formation during the growth of alluvial fans with supercritical distributaries. *Sedimentology*, 60(6), 1498–1525. <https://doi.org/10.1111/sed.12046>Harvey, A. M. (2010). Local buffers to the sediment cascade: debris cones and alluvial fans. In T. P. Burt & R. J. Allison (Eds.), *Sediment Cascades: An Integrated Approach* (pp. 153–180). West Sussex, UK: Wiley-Blackwell.Hijmans, R. J., Etten, J. van, Sumner, M., Cheng, J., Bevan, A., Bevan, R., ... Greenberg, J. A. (2020). *Geographic Data Analysis and Modeling* (pp. 1–249). pp. 1–249. Retrieved from <https://cran.r-project.org/web/packages/raster/raster.pdf>Hooke, R. L. (1967). Processes on Arid-Region Alluvial Fans. *The Journal of Geology*, 75(4), 438–460. <https://doi.org/10.1086/627271>Hooke, R. L. (1968). Steady-state relationships on arid-region alluvial fans in closed basins. *American Journal of Science*, 266, 609–629.Hooke, R. L., & Rohrer, W. L. (1979). Geometry of alluvial fans: Effect of discharge and sediment size. *Earth Surface Processes*, 4(2), 147–166. <https://doi.org/10.1002/esp.3290040205>Iverson, R. M. (1997). The Physics of Debris Flows. *Review of Geophysics*, 35(3), 245–296.Jakob, M. (1996). *Morphometric and geotechnical controls of debris flow frequency and magnitude in southwestern British Columbia*. University of British Columbia.Jakob, M. (2021). Landslides in a Changing Climate. In T. Davies & N. J. Rosser (Eds.), *Landslides: Hazards, Risks and Disasters* (In print).Jakob, M., & Church, M. (2020). The trouble with fans. *Innovation*, (July/August), 28–33.Jakob, M., & Lambert, S. (2009). Geomorphology Climate change effects on landslides along the southwest coast of British Columbia. *Geomorphology*, 107(3–4), 275–284. <https://doi.org/10.1016/j.geomorph.2008.12.009>Jakob, M., McDougall, S., Weatherly, H., & Ripley, N. (2013). Debris-flow simulations on Cheekye River, British Columbia. *Landslides*, 10, 685–699. <https://doi.org/10.1007/s10346-012-0365-1>Jakob, M., & Owen, T. (2021). Projected Effects of Climate Change on Shallow Landslides, North Shore Mountains, Vancouver, Canada. *Geomorphology*, In print.Jakob, M., Weatherly, H., Bale, S., Perkins, A., & Macdonald, B. (2017). A Multi-Faceted Debris-Flood Hazard Assessment for Cougar Creek, Alberta, Canada. *Hydrology*, 4(7), 1–34. <https://doi.org/10.3390/hydrology4010007>Kellerhals, R., & Church, M. (1990). *Alluvial fans. A field approach*. Chichester, NY: Wiley.Kim, W., & Jerolmack, D. J. (2008). The pulse of calm fan deltas. *Journal of Geology*, 116(4), 315–330. <https://doi.org/10.1086/588830>Lau, C. C. A. (2017). *Channel Scour on Temperate Alluvial Fans in British Columbia*. Simon Fraser University.Leduc, P., Peirce, S., & Ashmore, P. (2019). Short communication: Challenges and applications of structure-from-motion photogrammetry in a physical model of a braided river. *Earth Surface Dynamics*, 7(1), 97–106. <https://doi.org/10.5194/esurf-7-97-2019>Leenman, A. (2021). *Environmental variability and geomorphic responses on alluvial fans*. The University of British

Columbia. Leenman, A., & Eaton, B. (2021). Mechanisms for avulsion on alluvial fans: insights from high-frequency topographic data. *Earth Surface Processes and Landforms*. <https://doi.org/10.1002/esp.5059>

Malverti, L., Lajeunesse, E., & Métivier, F. (2008). Small is beautiful: Upscaling from microscale laminar to natural turbulent rivers. *Journal of Geophysical Research: Earth Surface*, *113*(4), 1–14. <https://doi.org/10.1029/2007JF000974>

Miller, K. L., Kim, W., & McElroy, B. (2019). Laboratory Investigation on Effects of Flood Intermittency on Fan Delta Dynamics. *Journal of Geophysical Research: Earth Surface*, *124*(2), 383–399. <https://doi.org/10.1029/2017JF004576>

Morgan, J. A., Brogan, D. J., & Nelson, P. A. (2017). Application of Structure-from-Motion photogrammetry in laboratory flumes. *Geomorphology*, *276*, 125–143. <https://doi.org/10.1016/j.geomorph.2016.10.021>

Pacheco-Ceballos, R. (1984). Energy losses and shear stresses in channel bends. *Journal of Hydraulic Engineering*, *110*(9), 1281–1284. [https://doi.org/10.1061/\(ASCE\)0733-9429\(1984\)110:9\(1282\)](https://doi.org/10.1061/(ASCE)0733-9429(1984)110:9(1282))

Paola, C., Straub, K., Mohrig, D., & Reinhardt, L. (2009). The “unreasonable effectiveness” of stratigraphic and geomorphic experiments. *Earth-Science Reviews*, *97*(1–4), 1–43. <https://doi.org/10.1016/j.earscirev.2009.05.003>

Parker, G., Paola, C., Whipple, K. X., & Mohrig, D. (1998). Alluvial fans formed by channelized fluvial and sheet flow. I: Theory. *Journal of Hydraulic Engineering*, *124*(10), 985–995. [https://doi.org/10.1061/\(ASCE\)0733-9429\(1998\)124:10\(985\)](https://doi.org/10.1061/(ASCE)0733-9429(1998)124:10(985))

Pierson, T. (2005). Hyperconcentrated flow — transitional process between water flow and debris flow. In *Debris-flow hazards and related phenomena* (pp. 159–202). Springer Berlin Heidelberg: Praxis Publishing Ltd.

Piliouras, A., Kim, W., & Carlson, B. (2017). Balancing Aggradation and Progradation on a Vegetated Delta: The Importance of Fluctuating Discharge in Depositional Systems. *Journal of Geophysical Research: Earth Surface*, *122*(10), 1882–1900. <https://doi.org/10.1002/2017JF004378>

Core Team. (2019). *R: A Language and Environment for Statistical Computing*. Retrieved from <https://www.r-project.org/Reitz>, M. D., & Jerolmack, D. J. (2012). Experimental alluvial fan evolution: Channel dynamics, slope controls, and shoreline growth. *Journal of Geophysical Research: Earth Surface*, *117*(2), 1–19. <https://doi.org/10.1029/2011JF002261>

Reitz, M. D., Jerolmack, D. J., & Swenson, J. B. (2010). Flooding and flow path selection on alluvial fans and deltas. *Geophysical Research Letters*, *37*(6), 1–6. <https://doi.org/10.1029/2009GL041985>

Roussel, J.-R., & Auty, D. (2020). *lidR: Airborne LiDAR Data Manipulation and Visualization 923 for Forestry Applications*. Retrieved from <https://cran.r-project.org/package=lidR>

Schumm, S. A., Mosley, M. P., & Weaver, W. (1987). *Experimental fluvial geomorphology*. New York: Wiley.

Takahashi, T. (2014). *Debris Flow: Mechanics, Prediction and Countermeasures* (2nd ed.). Boca Raton, FL: Taylor & Francis Group.

Turkington, T., Remaître, A., Etema, J., Hussin, H., & van Westen, C. (2016). Assessing debris flow activity in a changing climate. *Climatic Change*, *137*(1–2), 293–305. <https://doi.org/10.1007/s10584-016-1657-6>

Wasklewicz, T., & Scheinert, C. (2016). Development and maintenance of a telescoping debris flow fan in response to human-induced fan surface channelization, Chalk Creek Valley Natural Debris Flow Laboratory, Colorado, USA. *Geo-*

morphology, 252, 51–65. <https://doi.org/10.1016/j.geomorph.2015.06.033>Webb, R. H., Magirl, C. S., Griffiths, P. G., & Boyer, D. E. (2008). Debris Flows and Floods in Southeastern Arizona from Extreme Precipitation in July 2006 - Magnitude, Frequency, and Sediment Delivery. *U.S. Geological Survey, Open-File Report 2008-1274, 2008-1274*. Retrieved from <https://pubs.er.usgs.gov/publication/ofr20081274>Whipple, K. X., Parker, G., Paola, C., & Mohrig, D. (1998). Channel dynamics, sediment transport, and the slope of alluvial fans: Experimental study. *Journal of Geology*, 106(6), 677–693. <https://doi.org/10.1086/516053>Wilford, D., Sakals, M. E., Innes, J. L., & Sidle, R. (2004). Recognition of debris flow , debris flood and flood hazard through watershed morphometrics Recognition of debris flow , debris flood and flood hazard through watershed morphometrics. *Landslides*, 1(March), 61–66. <https://doi.org/10.1007/s10346-003-0002-0>Zarn, B., & Davies, T. R. H. (1994). The significance of processes on alluvial fans to hazard assessment. *Zeitschrift Fuer Geomorphologie*, 38(4), 487–500.